Optimization and Validation of a Human Ex Vivo Femoral Head Model for Preclinical Cartilage Research and Regenerative Therapies

Optimisation and validation of a human *ex vivo* femoral head model for pre-clinical cartilage research and regenerative therapies.

Katarzyna Styczynska-Soczka,[1] Anish K. Amin,[2] A. Hamish W. Simpson,[2] Andrew C. Hall.[1]

[1]Edinburgh Medical School: Biomedical Sciences,
Hugh Robson Building,
George Square,
Edinburgh EH8 9XD, U.K.

[2]Department of Trauma and Orthopaedic Surgery,
Royal Infirmary of Edinburgh,
49 Little France Crescent,
Edinburgh EH16 4SA, U.K.

Correspondence to:

Dr Andrew C. Hall
Edinburgh Medical School: Biomedical Sciences,
University of Edinburgh,
Hugh Robson Building,
George Square,
Edinburgh EH8 9XD,
Scotland, U.K.
Phone + 44 (0)131 650 3263
FAX + 44 (0)131 650 2872
E.mail; a.hall@ed.ac.uk

Key words:
Femoral head, articular cartilage, chondrocytes, disuse atrophy, phenotype.

Abstract:

Objective. Articular cartilage is incapable of effective repair following injury or during osteoarthritis. While there have been developments in cartilage repair technologies, there is a need to advance biologically-relevant models for pre-clinical testing of biomaterial and regenerative therapies. This study describes conditions for the effective *ex vivo* culture of the whole human femoral head.

Design. Fresh, viable femoral heads were obtained from femoral neck fractures and cultured for up to 10wks in: (a) Dulbecco's modified Eagle's medium (DMEM); (b) DMEM+mixing; (c) DMEM+10% human serum (HS); (d) DMEM+10%HS+mixing. The viability, morphology, volume and density of fluorescently-labelled *in situ* chondrocytes and cartilage surface roughness were assessed by confocal microscopy. Cartilage histology was studied for glycosaminoglycan content using Alcian blue and collagen content using picrosirius red.

Results. Chondrocyte viability remained at >95% in DMEM+10%HS. In DMEM alone, viability remained high for ~4wks then declined. For the other conditions, superficial zone chondrocyte viability fell to <35% at 10wks with deeper zones being relatively unaffected. In DMEM+10% HS at 10wks, the number of chondrocytes possessing cytoplasmic processes increased compared to DMEM (p=0.017). Alcian blue labelling decreased (p=0.02) and cartilage thinned (p≤0.05), however there was no change to surface roughness, chondrocyte density, chondrocyte volume, or picrosirius red labelling (p>0.05).

C*onclusions*. In this *ex vivo* model, chondrocyte viability was maintained in human femoral heads for up to 10wks in culture, a novel finding not previously reported. This human model could prove invaluable for the exploration, development and assessment of pre-clinical cartilage repair and regenerative therapies.

Introduction:

Articular cartilage has very poor regenerative potential following injury and the repair tissue formed is mechanically weak, and has a fibro-cartilageneous, rather that the resilient load-bearing extracellular matrix (ECM) of hyaline cartilage[1]. Furthermore, the native regeneration potential of cartilage declines with age[2] and while fibro-cartilaginous repair can be observed to form within injured hyaline cartilage, it is more evident when the injury has penetrated the sub-chondral bone.[1,3] The reasons for the production of mechanically-incompetent repair tissue are not well understood, and clearly there is intense interest in developing more effective biomaterial and regenerative therapies for cartilage repair. However, current models are not optimal and usually involve preparations ranging from *in vitro* cultures of cells, through to osteochondral explants[4] and *ex vivo* and *in vivo* models of mainly animal (i.e. non-human) joints[5,6]. The research and development of more effective cartilage repair and regenerative therapies would be enhanced by the ability to pre-clinically evaluate novel strategies in *ex vivo* physiological, tribological models of natural joints.

While there have been many detailed studies on explant and organ culture of animal osteochondral tissue (e.g.[7]), few studies have conducted experiments directly on human tissue. The limited studies using human cartilage for experimentation have obtained the material as discarded, and frequently degenerate osteochondral tissue (e.g. during joint replacement surgery for osteoarthritis)[8]. To test orthobiological treatments for human cartilage repair, the use of healthy cartilage is essential. However, this source of material is difficult to obtain and relies on collaboration between clinicians, theatre staff and research scientists. Whilst normal human cartilage may be obtained from amputations, trauma victims or occasionally cadavers, such material is rarely available for wider adoption into experimental human cartilage research. *Ex vivo* organ culture is becoming increasingly important for basic and applied biomedical research because it is more representative of normal cellular behaviour. However, obtaining a steady supply of viable human tissue which then has to be cultured for weeks under aseptic conditions remains a challenging research area.

Femoral neck fractures are one of the most common surgically treated injuries in elderly patients. The human femoral head is discarded during the surgery undertaken to treat femoral neck fractures and is replaced with an artificial prosthesis. While this discarded femoral head is aged, it is generally non-degenerate. We hypothesised that the human femoral head would be a viable source

of normal, non-degenerate articular cartilage suitable for pre-clinical cartilage research and regenerative therapies. We were able to coordinate the timely, sterile collection and delivery of the discarded human femoral head from the operating theatre to the laboratory. The aim of this study was to optimise the culture conditions for fresh human femoral heads from femoral neck fractures to permit viable long-term (10wk) culture.

Methods

Human femoral heads

Femoral heads were obtained with ethical permission (Tissue Governance, National Health Service, Lothian) and patient consent from 15 patients (11 females, 4 males, mean age 75.5 (range 56-88)) undergoing hemi-arthroplasty or total hip replacement for femoral neck fracture (FNF). Femoral heads were carefully removed intra-operatively by a qualified orthopaedic surgeon using a corkscrew device and immediately placed into a sterile container with saline (0.9% w/v;21^{o}C) to prevent chondrocyte death from drying[9]. Femoral heads were then transferred to a sterile container with Dulbecco's Modified Eagle's Medium (DMEM) with D-glucose (25mM), L-Glutamine (4mM), pyruvate (1mM), 100U/ml penicillin, 100µg/ml streptomycin, 2.5mg/ml amphotericin B (Sigma-Aldrich, Irvine, UK) and 10µg/ml Fungin (InvivoGen, Toulouse, France) ready for transportation to the laboratory with the femoral heads being available for experiments within 1-2hrs.

Culture conditions

Femoral heads were maintained in culture (37^{o}C) in sealed single use sterile containers and media changed every 3 days and the container replaced with every media change. Media volume for each femoral head was ~50-60ml. Male femoral heads were larger than those of females (diam. typically 6cm *vs* 4.5cm) and required larger culture containers. The femoral heads were cultured for up to 10 weeks under the following conditions: (a) static culture in Dulbecco's modified Eagle's medium (DMEM), (b) culture in DMEM with movement (DMEM+mixing), (c) as for (a) above +10% normal human serum (HS, Merck, Feltham, U.K) and (d) as for (b) above +10% HS. A cavity was carved in the cancellous bone of the femoral head for a magnetic stirring bar using bone trimmers (Fig. 1). Containers were then placed on a magnetic mixer inside the incubator and stirring was programmed for 1h, twice daily at ~1Hz. The rationale for studying the effects of movement was based on our proof of concept bovine model where joint movement promoted chondrocyte viability[7].

Cartilage sampling, fluorescent labelling of in situ chondrocytes and confocal microscopy

Full depth cartilage explants were harvested using 3 or 5mm diam. biopsy punches (Kai Medical, Solingen, Germany) for weekly chondrocyte viability measurements. To minimise the variability, explants were taken from random areas within the load-bearing parafoveal superior region[10] (Fig. 2). Cartilage samples were then incubated (1.5h;21°C) with CMFDA (5-chloromethylfluorescein diacetate) cell tracker green and PI propidium iodide (12.5 and 10μM, respectively; Invitrogen, Paisley, U.K.) to label living (green) and dead (red) cells respectively[11]. Explants were washed in phosphate-buffered saline (PBS; Invitrogen, Paisley, U.K.), fixed (formaldehyde 4%v/v;30mins; Fisher, Leicestershire, U.K.) and imaged in three-dimensions by confocal laser scanning microscopy (CLSM) using established methods[12].

Measurements of chondrocyte viability, density, volume and morphology

Confocal projected axial views were analysed using ImageJ/FIJI (National Institutes of Health) and IMARIS software (Zurich, Switzerland) as described[12]. Chondrocyte viability (% live cells) was calculated as: the number of CMFDA-labelled cells/(number of CMFDA-labelled cells + number of PI-labelled cells) in a given Region of Interest (ROI) volume. For chondrocyte density, the total number of cells (CMFDA-labelled and PI-labelled) in the ROI volume were counted in IMARIS, and results given as cells/μm^3. Chondrocyte volumes were obtained using the IMARIS 'Surfaces' algorithm. Volume calibration was performed using fluorescent microspheres (Polysciences, Warrington, USA). Chondrocyte morphology was considered 'normal' if cells were visualised as having a 'smooth' surface and elliptical/rounded shape. 'Abnormal' chondrocytes exhibited at least one CMFDA-labelled cytoplasmic process ≥2μm long. Abnormal cells were counted manually and divided by the total number of live cells in the field of view with results presented as the % abnormal cells in the whole cell population within the ROI[12].

Histology, cartilage thickness and surface roughness

Explants were frozen (-80°C) in a freezing medium (1:1 Optimal temperature cutting compound with 30% w/v sucrose in PBS for histology[13,14]. The plugs were then cut into 40μm sections and stained with Alcian blue (Vector Laboratories Ltd., Peterborough, U.K.) to label cartilage glycosaminoglycans according to manufacturer's instructions. For picrosirius red staining of

collagens, sections of 10µm thickness were first stained with haematoxylin for 8mins, then washed 3-4x in distilled water. This was followed by 1h incubation in 0.1% picrosirius red (Direct Red 80, Sigma-Aldrich, Irvine, U.K.) in picric acid (VWR International, Lutterworth, U.K.). Sections were washed briefly 2x in 0.5% acetic acid, dehydrated (two washes in ethanol absolute followed by one wash in xylene) and mounted in resinous mounting medium. Histological sections were imaged on a Leica bright field microscope and analysed with ImageJ/FIJI software[15]. After converting the images to greyscale 8-bit pixel depth, the same intensity threshold was set for each pair of sections (week 0 *vs* week 10). The stained area above the threshold was measured and presented as a % of the total sectional area. Cartilage thickness measurements were performed on the coronal sections of cartilage using ImageJ/FIJI. For the surface roughness measurements, the ImageJ/FIJI Analyse Stripes macro was used on the images of histologically-stained sections. Calculation of cartilage surface roughness was based on the deviation from an idealized smooth cartilage surface, and expressed as Rq (the root mean square (RMS) deviation) in µm.

Data presentation and statistical analysis

Statistical analyses were performed using Graphpad Prism ver.8.2.1 (GraphPad Software, La Jolla, U.S.A.). Data were presented as (N(n)), with (N) representing the number of independent femoral heads and (n) the total number of replicates. Each data point presented on graphs and used for statistical analyses was an average (± S.D. or S.E.M. as indicated) of the replicates taken from each femoral head. Unless otherwise stated, paired Student's t-tests were used to compare differences within pairs of treatment groups or time points, and ANOVA used to compare differences across several groups. A significant difference was accepted when $p<0.05$.

Results

Cartilage grading and chondrocyte viability

Femoral heads were macroscopically assessed using an established system[16]. For all femoral heads considered suitable, the cartilage was grade 0 over >75% of the surface, with small isolated grade 1 lesions in the parafoveal area (which were <25% of the surface area). The isolated areas of grade 1 cartilage (mild surface fibrillation) were not studied and only cartilage of grade 0 was used.

Chondrocyte viability was assessed on day 1 and any femoral heads with a viability of <80% were excluded. Out of a total of 24 femoral heads received, five were excluded due to low initial chondrocyte viability and a further four were also excluded as they developed infection during subsequent culture. In the remaining 15 femoral heads, the cell viability was 95.3±5.3% (N(n)=15(60)) on Day 1. Chondrocyte viability in femoral heads cultured under static conditions in DMEM remained high (>90%) for ~4wks but decreased to 44.0±22.3% by week 10 (N(n)=4(16), one-way ANOVA, post-test for trend, p=0.045, Fig. 3A). This decrease in cell viability was accelerated with movement of the femoral head and stirring of the media with virtually no viable cells by week 6 (two-way ANOVA;p=0.0099, Fig. 3A). The addition of 10% HS to DMEM maintained chondrocyte viability at >90% to week 10 under static femoral head culture conditions (Fig. 3B) but did not significantly improve the viability in femoral head cultures with movement/stirring over 10 weeks.

CLSM permits three-dimensional imaging and quantitative analyses of chondrocyte viability within the full depth of cartilage[17]. To assess if chondrocytes within any zone were more sensitive during culture, chondrocyte viability was determined as a function of depth from the articular surface. We compared the percentage cell viability within the different zones (SZ, MZ, DZ) in coronal sections of articular cartilage at week 10 compared with baseline (week 0). There was a decrease in the SZ viability in both culture conditions (DMEM only, and DMEM+mixing; (p=0.0425 and p=0.016 respectively; Fig. 4A)) with relative preservation of cell viability in deeper cartilage zones (Fig. 4B). This suggest that SZ chondrocytes were far more sensitive to the culture conditions compared to the cells in the deeper zones. Thus, although there were few living SZ cells remaining after 10wks, a substantial portion of chondrocytes in the other zones were still viable.

Chondrocyte morphology

In fresh explants of macroscopically non-degenerate femoral head cartilage, a small population (8.0±1.5% (N(n)=4(8)) of cells in the SZ (~100µm from the surface) demonstrated one or more cytoplasmic processes (Fig 5. A,B). During femoral head culture in DMEM, there appeared to be an increase in the % of cells with processes (to 15±5.3% by week 6, N(n)=4(16)) and (16±6.4% by week 10 N(n)=4(16)) however these changes were not significantly different compared to week 0 (ANOVA;p>0.05). In contrast, in the presence of HS, the % of chondrocytes with processes increased to 31±9.3% by week 6 (p=0.008;N(n)=3(12)) and 37±7.1% by week 10 (p=0.002;N(n)=3(12)) compared to week 0 (Fig. 5B). By week 10, there were significantly more (by >2-fold;p=0.017) chondrocytes with cytoplasmic processes when femoral heads were cultured in DMEM+HS compared to DMEM alone (Fig. 5B).

Extracellular matrix composition

To evaluate whether extracellular matrix composition changed during culture, two histological stainings were performed on cartilage samples (week 0 and week 10) and analysed semi-quantitatively. There was a general trend of decreasing GAG staining using Alcian blue[18] under all culture conditions, but in DMEM+HS chondrocyte viability was significantly higher (Fig. 6A). In these cultures 50.0±2.86% (N(n)=3(6)) of the section area was stained with Alcian blue at week 0. This decreased to 17.0±13.8% by week 10 (N(n)=3(6);p=0.028)). The total collagen stained with picrosirius red did not show any significant difference between DMEM and DMEM+HS samples at week 0 and week 10 (30±5% *vs* 42±22%, N(n)=11(22);p=0.09). These results suggest a significant loss of GAGs but no change to the total collagen content of femoral head cartilage during this culture period.

Cartilage thickness and surface roughness

In parallel with the loss of GAGs, cartilage thickness was reduced after 10wks in culture (Fig. 6B). In DMEM cultures, it decreased from 3808±425µm to 2828±542µm (p=0.05;N(n)=4(22)). In the DMEM+mixing culture it declined from 4226±418µm to 2703±720µm (p=0.02;N(n)=4(15)), and in

DMEM+10% human serum it decreased from 3377±360µm to 2349±160µm (p=0.02;N(n)=3(22)). Articular surface roughness assessed on the same femoral heads at week 0 and week 10 was not significantly different (13±0.6µm and 15±0.7µm respectively (p=0.55;N(n)=9(9);Fig. 7A)).

Chondrocyte density and volume

There was no difference in cell density for all the samples at week 0 (9971±2389 cells/mm^3 N(n)=15(60)) compared with week 10 (11256±3305 cells/mm^3 (p=0.01;N(n)=15(60));Fig 7B)). *In situ* chondrocyte volume was also analysed as it correlates with the progression of cartilage degeneration, however, there was no difference (p=0.22) between the cell volumes of chondrocytes on day 0 (423±49µm^3, N(n)=15(60) and week 10 (441±48µm^3, N(n)=15(60);Fig. 7C).

Discussion.

We have established culture conditions which maintain chondrocyte viability during *ex vivo* culture of human femoral heads for 10 weeks by supplementing standard culture medium with 10% normal human serum. We have identified an excellent and reliable source of viable, non-degenerate human articular cartilage ideal for *ex vivo* experimentation. Previously, we have investigated the microscopic effects of mechanical and other forms of injury on human articular cartilage[9,19]. However material was obtained from tissue discarded during knee replacement for osteoarthritis and the yield of non-degenerate tissue was often low. This was because the majority of the tissue was osteoarthritic with loss of superficial zone cells, even if macroscopically the tissue may have appeared non-degenerate. In contrast, the cartilage of the femoral head discarded after femoral neck fracture was in most cases non-degenerate and our experiments have confirmed the presence of viable cartilage tissue that is macroscopically and microscopically ideally suited for investigating cartilage repair and regeneration. Due to the excellent chondrocyte viability throughout culture, the model may also allow *ex vivo* validation of an optimal combination of cells, growth factors and scaffolds that lead to the formation of repair tissue resembling the desirable hyaline articular cartilage at the microscopic level.

Current knowledge of the microscopic quality of cartilage repair tissue in humans is based on histological assessment of opportunistic biopsy specimens retrieved during 'second look' arthroscopy (keyhole surgery). While these specimens have provided valuable insight into the quality of cartilage repair, with so called 'hyaline-like' composition, the information is limited by small numbers of specimens, distortion of the tissue during biopsy, variability in the site/size of biopsies and heterogeneity of the study sample. The lack of a non-invasive method of evaluating the microscopic characteristics of the quality of the cartilage repair tissue has also been recognized as a major problem limiting advances in cartilage repair and regenerative techniques by the International Cartilage Repair Society (ICRS)[20]. Modern imaging techniques (e.g. CLSM) allow microscopic examination of articular cartilage by optically sectioning the tissue. We believe that the significantly easier access to normal, human cartilage *ex vivo* will help overcome the problems associated with *in vivo* biopsy, and allow detailed quantitative microscopic assessment and

optimisation of the quality of cartilage repair. The proposed model will significantly enhance our ability to test a wide range of pre-clinical therapeutic cartilage repair and regenerative strategies directly in human tissue so that the best candidate therapies can be identified for subsequent clinical study.

In our model, the large area of grade 0 cartilage (Fig. 1) permitted multiple samples to be taken either at a single time point, or a smaller number over a longer time course. A gap between samples was retained so that cutting trauma using the biopsy punch[21] did not influence neighbouring samples. Furthermore, if cartilage wells were to contain biological models for testing, then it would be possible for the full depth sample to be 'scooped' out using a fine scalpel blade. Chondrocyte viability in both axial and coronal projections was initially high for all samples (Fig. 3A). There was no change in viability during DMEM+HS culture, suggesting that taking multiple cartilage plugs over the 10wk period did not adversely affect the viability of the surrounding cartilage. It should be noted that if serum (HS) was used, then it must be heat-treated because it contains enzymes that digest the DNA of dead cells leading to an under-estimation of the dead cell population[22,23].

Femoral head culture in DMEM maintained chondrocyte viability for ~4wks after which there was an increase in chondrocyte death (Fig. 3A). With mixing, viability decreased progressively after the start of the culture, such that by week 10 there were virtually no remaining viable cells. Furthermore, cell death started in the SZ so that after 10wks, all these chondrocytes were dead whereas those in the deeper zones were still viable (Fig. 4). This suggests that there are factors in bone supporting chondrocyte viability in the superficial zone which were washed out during media changes. The importance of bone in cultures of bovine cartilage has been reported previously as SZ chondrocyte viability was maintained in cartilage cultures when bone was present either when attached to the explants or in co-culture[24]. This was in contrast to deep zone chondrocytes which survived, and the relative viability of these chondrocytes within the femoral head cartilage of our elderly patients (Fig. 4) parallels the long-term (~25yr) survival of DZ chondrocytes in osteochondral allografts used for the treatment of focal post-traumatic defects in young individuals[25]. It is possible that these chondrocytes are well adapted to this relatively hostile environment for example chondrocytes in the DZ utilise different membrane transport systems for the regulation of intracellular acidity compared to cells in the SZ[26]. The addition of HS in the mixed DMEM condition provided

some protection for SZ chondrocytes as cell viability by week 10 was 35% (Fig. 3B). However, if there was no mixing and HS was present, there was complete chondrocyte protection suggesting that serum was protecting the cells which were vulnerable during the latter stages of the culture. While the cross-talk between subchondral bone and cartilage has received considerable attention[27] the factor(s) released from bone and/or present in the serum which promote chondrocyte viability are unclear, with TGFβ, IGF-1 and BMP being implicated[28].

Visualisation of fluorescently-labelled *in situ* chondrocytes revealed the classical morphology of elliptical cells in the SZ with the more spheroidal forms in the deeper zones (Fig. 4)[12]. In grade 0 cartilage in axial projections, a small proportion (~8%) of the SZ cells (within ~100μm depth). exhibited cytoplasmic processes. Of interest was that after 10wks of culture in DMEM+HS, there was a significant (>4-fold) increase in the % of cells exhibiting processes (Fig. 5A). At week 10, significantly (by >2-fold) more chondrocytes demonstrated a cytoplasmic process when HS was present compared to culture in DMEM alone. However, in the DMEM+HS condition, chondrocyte viability and density did not change during culture (Figs. 3B & 7B respectively), whereas in DMEM alone viability had decreased by ~50% (Fig. 3A) but abnormal chondrocytes were still present (Fig. 5B). The changes to chondrocyte shape might be related to the properties of the ECM. In healthy cartilage, the pore size of the PG network is ~3nm whereas that for collagen is ~100nm and thus the PGs will regulate cartilage permeability and solute diffusivity[29]. GAG loss during unloading will increase matrix permeability and thus potent growth factors etc., in serum will start to penetrate and act particularly on SZ chondrocytes which are normally shielded by the tight matrix. The development of processes and subsequent abnormal morphology of chondrocytes is a feature associated with de-differentiation to a fibroblastic phenotype[30,31] and has been observed in osteoarthritic tibial and femoral head cartilage[17,32,33]. A change in phenotype is characterised by decreased hyaline cartilage-specific collagen type II and aggrecan production, and an increase in collagen type I production. It would be of particular interest to determine if physiological levels of loading could reverse some of these changes and protect the chondrocyte phenotype and promote the production of a hyaline cartilage[17].

There was no evidence of chondrocyte clustering[34] under any of the experimental conditions. Nomura et al.[35] did not observe changes to chondrocyte morphology in mice subjected to hindlimb

unloading when cartilage was studied by histology. This might appear to conflict with the changes to chondrocyte morphology reported here. However the detection of the fine cytoplasmic process is not possible with their histological techniques as they involve tissue shrinkage[36] and high resolution imaging of unperturbed *in situ* chondrocyes is essential for the visualisation of the processes[17,31].

It might be considered that a limitation in our study was that no mechanical load was applied to the femoral heads. However this revealed that after 10wks there were features of the cartilage ECM and *in situ* chondrocytes which bear similarities to the changes observed with both *in vivo* and *in vitro* cartilage disuse atrophy. Alcian blue staining reflecting GAG content was decreased (Fig. 6A,C). This was not significant in the DMEM and DMEM+mixing conditions when there was substantial chondrocyte death (~50% and 100% respectivey). However, interestingly, the decrease was significant in the DMEM+HS condition (Fig.6A) when cell viability was high (>95%). This suggests that there was an active chondrocyte-driven process mediating reduced GAG levels[37]. GAG loss would probably account for the cartilage thinning (Fig. 6B), reported by others using animal joint immobilisation models[35]. GAG loss did not however, affect surface roughness (Fig. 7A) which is in contrast to the changes occurring in OA, where GAG levels decrease and surface roughness and cartilage fibrillation increase[28]. Palmoski *et al*.[38] noted a similar decrease in PG staining in healthy adult dogs after ~6 days of immobilisation and by 8wks there was a 30-50% reduction in cartilage thickness with an almost complete loss of PG. In human joints immobilised as a result of ankle fracture, there was a 6.6% loss of cartilage thickness over 7wks following fracture[39]. The loss of GAGs is thought to be due to a reduction in synthesis as well as the stimulation of chondrocyte degradative enzyme (MMP-13, ADAMTS5) activity[35,37] from a mechano-adaptive response to reduced load. Mechanical loading of joints is a key parameter for maintaining the differentiated, rounded, chondrocyte phenotype[40,41]. Recent studies implicate an essential role for the mechanosensitive ion channel Transient Receptor Potential Vanilloid 4 (TRPV4) in the signal transduction pathway. Inhibiting TRPV4 prevents loading-mediated increases in matrix synthesis, whereas activating TRPV4 in the absence of loading increases matrix synthesis in a manner analogous to loading[42].

While there were changes to GAG labelling, there was no change to picrosirius red labelling suggesting the cartilage collagen content remained unaltered throughout culture. While picrosirius

red does not discriminate between the collagen types[43] it is possible that there were changes to collagen metabolism and/or its organisation. For example, while total collagen content might not have change significantly, it is possible that there was a decrease in the collagen type II : type I ratio reflecting chondrocyte de-differentiation. In addition, changes to collagen fibre distribution/orientation could be evident, and future studies utilising polarized light microscopy would be worth pursuing. A small decrease in collagen cross-linking which recovers after re-mobilisation has been reported[44] and the immobilisation of rabbit knee joint leads to a partial shift in the density of collagen composition from type II to type I[45]. However, in human cartilage, there is negligible/minimal collagen turnover over the lifetime in a healthy joint[46].

There was no change to the volume of *in situ* chondrocytes following 10wks culture in DMEM+HS (Fig. 7C). It is likely that with the loss of GAGs, interstitial osmolarity of the matrix would decrease, leading to hypo-osmolarity and cell swelling. However *in situ* chondrocytes possess effective volume-regulatory channels and transporters[47,48] and over a long time period, despite the change in osmolarity, these mechanisms could compensate leading to no volume change. This phenomenon (termed iso-volumetric volume regulation (IVR)) has been described in various cell types including chondrocytes[49]. The lack of chondrocyte swelling is in contrast to that observed in osteoarthritic cartilage where increased chondrocyte volume/hypertrophy has been reported[17,50].

This study described the first successful *ex vivo* culture of a large human joint. *In situ* chondrocyte viability remained high in DMEM+HS, however it decreased under the other conditions tested. Although chondrocyte viability was optimal, there were changes to the matrix (cartilage thinning, GAG loss, no change to collagen or surface roughness) and chondrocytes (development of cytoplasmic processes, no change to volume or density). This pre-clinical model may be an invaluable addition for the assessment of human cartilage repair therapies and may replace some animal studies.

Acknowledgements.

We thank Ms F. Stewart for excellent assistance with the provision of the femoral heads, Dr A. Kubasik-Thayil at the IMPACT imaging facility in the Centre for expert assistance with confocal imaging, and Ms A. Luczak for assistance with histology.

Role of the Funding Source.

This work was supported by a project grant from the Chief Scientist's Office (Scotland) TCS/18/01.

Author Contributions.

Study concept and design; Amin, Simpson, Hall. Acquisition of data; Styczynska-Soczka. Analysis and interpretation of data; Styczynska-Soczka, Amin, Simpson, Hall. Manuscript preparation; Styczynska-Soczka, Amin, Simpson, Hall.

Conflict of Interest.

The authors have no conflicts of interest to declare.

References.

1. Hunziker EB, Lippuner K, Keel MBJ, Shintani N. An educational review of cartilage repair: precepts & practice - myths & misconceptions - progress & prospects. Osteoarthritis and Cartilage 2015;23:334-350 http://dx.doi.org/10.1016/j.joca.2014.12.011

2. Brittberg M, Gomoll AH, Canseco JA, Far J, Lind M, Hui J. Cartilage repair in the degenerative ageing knee. Acta Orthopaedica 2016;87:sup363, 26-38, DOI: 10.1080/17453674.2016.1265877

3. Simon TM, Aberman HM. Cartilage regeneration and repair testing in a surrogate large animal model. Tissue Eng Part B Rev 2010;16:65-79. DOI: 10.1089/ten.TEB.2009.0304.

4. Maglio M, Tschon M, Sicuro L, Lolli R, Fini M. Osteochondral tissue cultures: between limits and sparks, the next step for advanced in vitro models. J Cell Physiol 2018;234:5420-5435. DOI: 10.1002/jcp.27457

5. Elson KM, Fox N, Tipper JL, Kirkham J, Hall RM, Fisher J, *et al,* Non-destructive monitoring of viability in an ex vivo organ culture model of osteochondral tissue. Europ Cells Mat 2015;29:356-369. DOI: 10.22203/eCM.v029a27

6. Cope PJ, Ourradi K, Li Y, Sharif M. Models of osteoarthritis: the good, the bad and the promising. Osteoarthritis and Cartilage 2019;27:230-239. https://doi.org/10.1016/j.joca.2018.09.016

7. Lin Y-C, Hall AC, Simpson AHRW. A novel joint organ culture model for evaluation of static and dynamic load on articular cartilage. Bone & Joint Research 2018;7(3):205-212. DOI:10.1302/2046-3758.73BJR-2017-0320

8. Geurts J, Juric D, Müller M, Schären S, Netzer C. Novel ex vivo human osteochondral explant model of knee and spine osteoarthritis enables assessment of inflammatory and drug treatment responses. Int J Mol Sci 2018;19:1314. DOI: 10.3390/ijms19051314

9. Paterson SI, Amin AK, Hall AC. Airflow accelerates bovine and human articular cartilage drying and chondrocyte death. Osteoarthritis and Cartilage 2015;23:257-265. DOI: 10.1016/j.joca.2014.10.004.

10. Greenwald AS, Haynes DW. Weight-bearing areas in the human hip joint. J Bone Jt Surg (Br). 1972;54(1):157-63.

11. Amin AK, Bush PG, Huntley JS, Simpson AHW, Hall AC. Osmolarity influences chondrocyte death in wounded articular cartilage. J Bone Jt Surg (Amer) 2008;90:1531-1542. DOI: 10.2106/JBJS.G.00857

12. Karim A, Amin AK, Hall AC. The clustering and morphology of chondrocytes in normal and mildly-degenerate human femoral head cartilage studied by confocal laser scanning microscopy. J Anatomy 2018;232(4):686-698. DOI: 10.1111/joa.12768.

13. Hyllested JL, Veje K, Ostergaard K. Histochemical studies of the extracellular matrix of human articular cartilage - A review. Osteoarthritis and Cartilage 2002;10:333–343. https://doi.org/10.1053/joca.2002.0519

14. Schmitz N, Laverty S, Kraus VB, Aigner T. Basic methods in histopathology of joint tissues. Osteoarthritis Cartilage 2010;18:S113-S116. https://doi.org/10.1016/j.joca.2010.05.026

15. Crowe AR, Yue W. Semi-quantitative determination of protein expression using immunohistochemistry staining and analysis: An integrated protocol. Bio Protoc 2019;9(24) pii: e3465. DOI: 10.21769/BioProtoc.3465.

16. Pritzker KPH, Gay S, Jimenez SA, Ostergaard K, Peletier J–P, Revell PA, *et al* (2006). Osteoarthritis cartilage histopathology: grading and staging. Osteoarthritis and Cartilage 2006;13:13-29. DOI:10.1016/j.joca.2005.07.014

17. Bush PG, Hall AC. The volume and morphology of chondrocytes within non-degenerate and degenerate human articular cartilage. Osteoarthritis and Cartilage 2003;11(4):242-251. DOI:10.1016/s1063-4584(02)00369-2

18. Fisher M, Solursh M. Glycosaminoglycan localisation and role in maintenance of tissue spaces in the early chick embryo. J Embryol Exp Morphol 1977;42:195-207.

19. Amin AK, Huntley JS, Patton JT, Brenkel IJ, Simpson AHRW, Hall AC. Hyperosmolarity protects chondrocytes from mechanical injury in human articular cartilage. J Bone Joint Surg [Br] 2011;93-B:277-84. Doi: 10.1302/0301-620X.93B2.24977.

20. Hoemann C, Kandel R, Roberts S, Saris DB, Creemers L, Mainil-Varlet P et al. International Cartilage Repair Society (ICRS) Recommended Guidelines for Histological Endpoints for Cartilage Repair Studies in Animal Models and Clinical Trials. Cartilage 2011;2(2);153-72. Doi:10.1177/1947603510397535.

21. Huntley JS, McBirnie JM, Simpson AH, Hall AC. Cutting-edge design to improve cell viability in osteochondral grafts. Osteoarthritis and Cartilage 2005;13:665-671. DOI: 10.1016/j.joca.2005.04.007

22. Zhou S, Cui Z, Urban JPG. Dead cell counts during serum cultivation are under-estimated by the fluorescent live/dead assay. Biotechnol J 2011;6(5):513-518. DOI: 10.1002/biot.201000254.

487 23. Karim A, Hall AC. Hyperosmolarity normalizes serum-induced changes to chondrocyte
488 properties in a model of cartilage injury. Europ Cells Mat 2016;31:205-220. DOI:
489 10.22203/ecm.v031a14
490
491 24. Amin AK, Huntley JS, Simpson AHW, Hall AC. Chondrocyte survival in articular cartilage: the
492 influence of subchondral bone in a bovine model. J Bone Jt Surg (Br) 2009;91-B:691-699. DOI:
493 10.1302/0301-620X.91B5.21544
494
495 25. Gross AE, Kim W, Las Heras F, Backstein D, Safir O, Pritzker KP. Fresh osteochondral
496 allografts for posttraumatic knee defects: long-term followup. Clin Orthop Relat Res
497 2008;466(8):1863-70. DOI: 10.1007/s11999-008-0282-8.
498
499 26. Simpkin VL, Murray DH, Hall AP, Hall AC. Bicarbonate-dependent pH_i regulation by
500 chondrocytes within the superficial zone of bovine articular cartilage. J Cell Physiol 2007;212(3),
501 600-609. DOI: 10.1002/jcp.21054
502
503 27. Goldring SR, Goldring MB. Changes in the osteochondral unit during osteoarthritis: structure,
504 function and cartilage-bone crosstalk. Nat Rev Rheumatol 2016;12(11):632-644.
505 DOI: 10.1038/nrrheum.2016.148.
506
507 28. Loeser RF, Goldring SR, Scanzello CR, Goldring MB. Osteoarthritis: A disease of the joint as
508 an organ. Arth Rheum 2012;64(6):1697–1707. DOI:10.1002/art.34453
509
510 29. Graham BT, Wright AD, Burris DL, Axe MJ, Raisis LW, Price C. Quantification of solute
511 diffusivity in osteoarthritic human femoral head cartilage using correlation spectroscopy. J Orthop
512 Res 2018;36:3256-3267. DOI: 10.1002/jor.24138
513

514 30. Graceffa V, Vinatier C, Guicheux J, Stoddart M, Alini M, Zeugolis DI. Chasing chimeras – the
515 elusive stable chondrogenic phenotype. Biomaterials 2019;192:199–225.
516 https://doi.org/10.1016/j.biomaterials.2018.11.014
517
518 31. Hall AC. The role of chondrocyte morphology and volume in controlling phenotype –
519 implications for osteoarthritis, cartilage repair and cartilage engineering. Curr Top Rheumatol
520 2019;21:38 https://doi: 10.1007/s11926-019-0837-6
521
522 32. Holloway I, Kayser M, Lee DA, Bader DL, Bentley G, Knight MM. Increased presence of cells
523 with multiple elongated processes in osteoarthritic femoral head cartilage. Osteoarthritis and
524 Cartilage 2004;12:17–24. https://doi.org/10.1016/joca.2003.09.001.
525
526 33. Tesche F, Miosge N. New aspects of the pathogenesis of osteoarthritis: the role of fibroblast-
527 like chondrocytes in late stages of the disease. Histol Histopathol 2005;20:329–37. DOI:
528 10.14670/HH-20.329
529
530 34. Lotz MK, Otsuki S, Grogan SP, Sah R, Terkeltaub R, D'Lima D. Cartilage cell clusters. Arthritis
531 Rheum 2010;62:2206–2218. DOI: 10.1002/art.27528.
532
533 35. Nomura M, Sakitani N, Iwaawa H, Kohara Y, Takano S, Wakimoto Y, *et al.* Thinning of articular
534 cartilage after joint unloading or immobilization. An experimental investigation of the pathogenesis
535 in mice. Osteoarthritis and Cartilage 2017;25:727-736. DOI: 10.1002/jor.1100070305
536
537 36. Loqman MY, Bush PG, Farquharson C, Hall AC. A cell shrinkage artefact in growth plate
538 chondrocytes with common fixative solutions: importance of fixative osmolarity for maintaining
539 morphology. Eur. Cell. Mater. 2010;19:214-27. DOI:10.22203/ecm.v019a21
540
541 37. Grumbles RM, Howell DS, Howard GA, Roos BA, Setton LA, Mow VC, *et al.,* Cartilage
542 metalloproteinases in disuse atrophy. J Rheumatol Supp 1995;43:46-148.

543

544 38. Palmoski M, Perricone E, Brandt KD. Development and reversal of a proteoglycan aggregation
545 defect in normal canine knee cartilage after immobilization. Arth Rheum 1979;22:508–517.

546

547 39. Behrens F, Kraft EL, Oegema TR Jr. Biochemical changes in articular cartilage after joint
548 immobilization by casting or external fixation. J Orthop Res 1989;7(3):335-343. DOI:
549 10.1002/jor.1100070305

550

551 40. Sanchez-Adams J, Leddy HA, McNulty AL, O'Conor CJ, Guilak F. The mechanobiology of
552 articular cartilage: bearing the burden of osteoarthritis. Curr Rheumatol Rep 2014;16(10):451.
553 DOI: 10.1007/s11926-014-0451-6.

554

555 41. Wuest SL, Calio M, Wernas T, Tanner S, Giger-lange C, Wyss F, *et al.* Influence of
556 mechanical unloading on articular chondrocyte dedifferentiation. Int J Molecular Sciences
557 2018;19(5). DOI: 10.3390/ijms19051289

558

559 42. O'Conor CJ, Leddy HA, Benefield HC, Liedtke WB & Guilak F. TRPV4-mediated
560 mechanotransduction regulates the metabolic response of chondrocytes to dynamic loading. Proc
561 Natl Acad Sci USA 2014;111:1316-1321. DOI: 10.1073/pnas.1319569111

562

563 43. Lattouf R, Younes R, Lutomski D, Naaman N, Godeau, G., Senni, K, *et al.* Picrosirius red
564 staining: A useful tool to appraise collagen networks in normal and pathological tissues. J
565 Histochem Cytochem 2014;62(10):751–758. DOI: 10.1369/0022155414545787

566

567 44. Haapala J, Arokoski JP, Hyttinen MM, Lammi M, Tammi M, Kovanen V, *et al.* Remobilization
568 does not fully restore immobilization induced articular cartilage atrophy. Clin Orthop Relat Res
569 1999;362:218–229.

570

45. Aldahmash AM, El Fouhil AF, Mohamed RA, Ahmed AM, Atteya M, Al Sharawy SA, *et al.* Collagen types I and II distribution: a relevant indicator for the functional properties of articular cartilage in immobilised and remobilised rabbit knee joints. Folia Morphol 2015;74(2):169–175. DOI: 10.5603/FM.2015.0027.

46. Heinemeier KM, Schjerling P, Heinemeier J, Møller MB, Krogsgaard MR, Grum-Schwensen T, *et al.* Radiocarbon dating reveals minimal collagen turnover in both healthy and osteoarthritic human cartilage. Sci Transl Med 2016;8:346ra90. DOI: 10.1126/scitranslmed.aad8335.

47. Bush PG, Hall AC. Regulatory volume decrease (RVD) by isolated and in situ bovine articular chondrocytes. J Cell Physiol 2001;187:304-14. DOI: 10.1002/jcp.1077

48. Lewis R, Feetham C, Barrett-Jolley R. Cell volume control in chondrocytes. Cell Physiol Biochem 2011;28:1111–22. DOI: 10.1159/000335847.

49. Wang Z, Irianto J, Kazun S, Wang W, Knight MM. The rate of hypo-osmotic challenge influences regulatory volume decrease (RVD) and mechanical properties of articular chondrocytes. Osteoarthritis and Cartilage 2015;23:289-299. http://dx.doi.org/10.1016/j.joca.2014.11.003

50. Gratal P, Mediero A, Sánchez-Pernaute O, Prieto-Potin I, Lamuedra A, Herrero-Beaumont, G, *et al.* Chondrocyte enlargement is a marker of osteoarthritis severity. Osteoarthritis and Cartilage 2019;27(8);1229-1234. DOI: 10.1016/j.joca.2019.04.013.

595

596 **Figure Legends.**

597

598 **Figure 1.** The cavity produced in the cancellous bone of the human femoral head to accommodate
599 the magnetic bar for stirring culture experiments.

600

601 **Figure 2. Localisation of the cartilage area on human femoral heads used for sampling. (A)**
602 Lateral view of the femoral head, fovea (F) on the upper left, **(B)** Top view of the femoral head, **(C)**
603 Femoral head with biopsy explants taken from within the specified zone. Scale bar represents 25mm.

604

605 **Figure 3. The viability of *in situ* human chondrocytes within femoral head cartilage cultured**
606 **under various conditions. (A)** DMEM N(n)=4(16); DMEM + mixing (N(n)=3(12)). **(B)** DMEM +
607 normal human serum (HS); (N(n)=3(12)), DMEM + mixing + human serum (N(n)=2(8)); error bars
608 represent S.E.M. (or S.D. for N=2). **(C)** Representative images of viability staining (CMFDA green –
609 live cells, PI red – dead cells) at week 10 for DMEM, DMEM + 10% human serum and DMEM +
610 mixing; scale bars represent 100µm.

611

612 **Figure 4. Viability of chondrocytes in various zones after 10 weeks of femoral head culture**
613 **(A)** Comparison of chondrocyte viability in the whole thickness *vs* superficial zone at week 10 of
614 culture. DMEM N(n)=4(16), **p*=0.0425, DMEM + mixing, N(n)=3(12), **p*=0.016 (data shown as mean
615 ± S.E.M.). **(B)** Representative coronal images of labelled chondrocytes within cartilage sections
616 cultured in DMEM on day 0 (left panel), and after 10 weeks of culture in DMEM + mixing + HS on
617 week 10 (right panel). The scale bars represent 100µm.

618

619 **Figure 5. Changes to the morphology of *in situ* femoral head chondrocytes during culture.**
620 Panel **(A)** shows the % of cells with cytoplasmic processes at three time points (weeks 0, 6 and 10)
621 in cultures with DMEM (N(n) = 4(16)) and DMEM + human normal human serum (HS) (N(n) = 3(12)).
622 (Data shown as mean ± S.D.). Panel **(B)** shows representative images of cell stained with CMFDA

cell tracker green to visualise chondrocyte morphology, and propidium iodide (PI) red to identify dead cells. The top row of images is from DMEM cultures, (left to right panels for weeks 0, 6 and 10 respectively), the bottom row of images for DMEM + human serum (left to right panels for weeks 0, 6 and 10 respectively. Note examples of chondrocytes with cellular processes indicated by white arrowheads. The scale bar represents 100µm.

Figure 6. Histology of femoral head cartilage with time in culture. (A) GAG content in various culture conditions, (a) DMEM N(n)=4(8), (b) DMEM + mixing N(n)=4(8), (c) DMEM + 10% human serum N(n)=3(6), **p*=0.028. **(B)** Cartilage thickness in various culture conditions, (a) DMEM N(n)=4(24), (b) DMEM + mixing N(n)=4(24), (c) DMEM + 10% human serum N(n)=3(18), (*p*=0.05; *p*=0.02; *p*=0.02 respectively). (Data shown as mean ± S.E.M.). **(C)** Representative images for Alcian blue staining of DMEM + human serum on week 0 (left panel) and week 10 (right panel).

Figure 7. Surface roughness, chondrocyte density and volume of *in situ* femoral head chondrocytes with time in culture in DMEM + HS. (A) Surface roughness expressed as the root mean square (RMS) deviation)) in µm at week 0 and week 10, N(n)=3(9), *p*=0.2). **(B)** Cell density (total number of chondrocytes per mm^3) at week 0 and week 10, N(n)=3(60), *p*=0.22. **(C)** Chondrocyte volume at week 0 and week 10, N(n)=3(44), *p*=0.22. Broken lines illustrate pairs of data at week 0 and week 10 for each femoral head. (Data shown as mean ± S.D.).

Figure 1.

(Styczynska-Soczka et al., 2020)

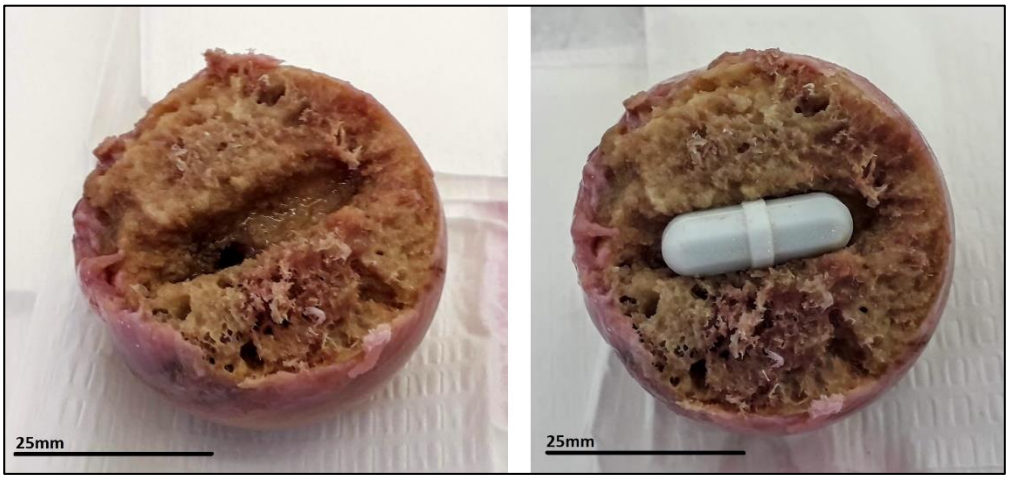

Figure 2.

(Styczynska-Soczka et al., 2020)

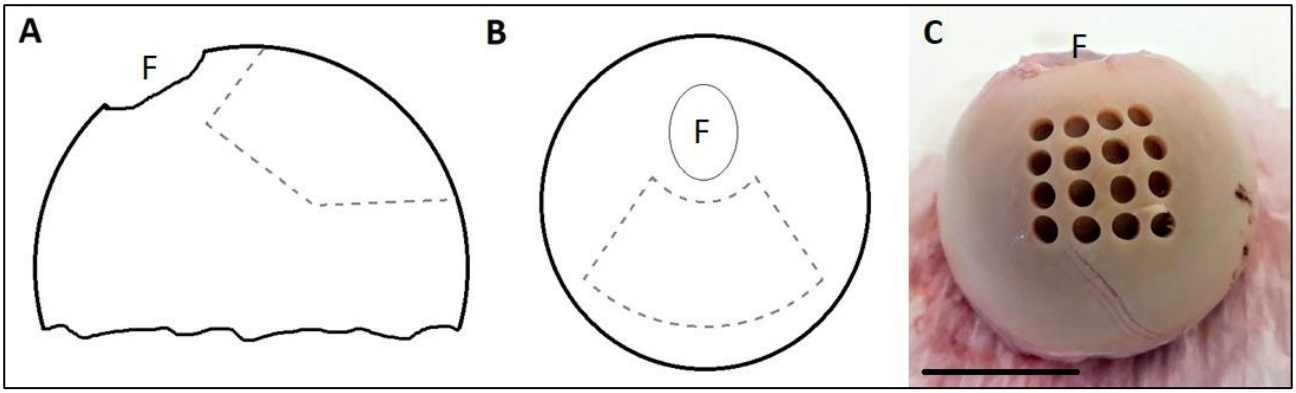

682 Figure 3.
683
684 (Styczynska-Soczka et al., 2020)
685
686

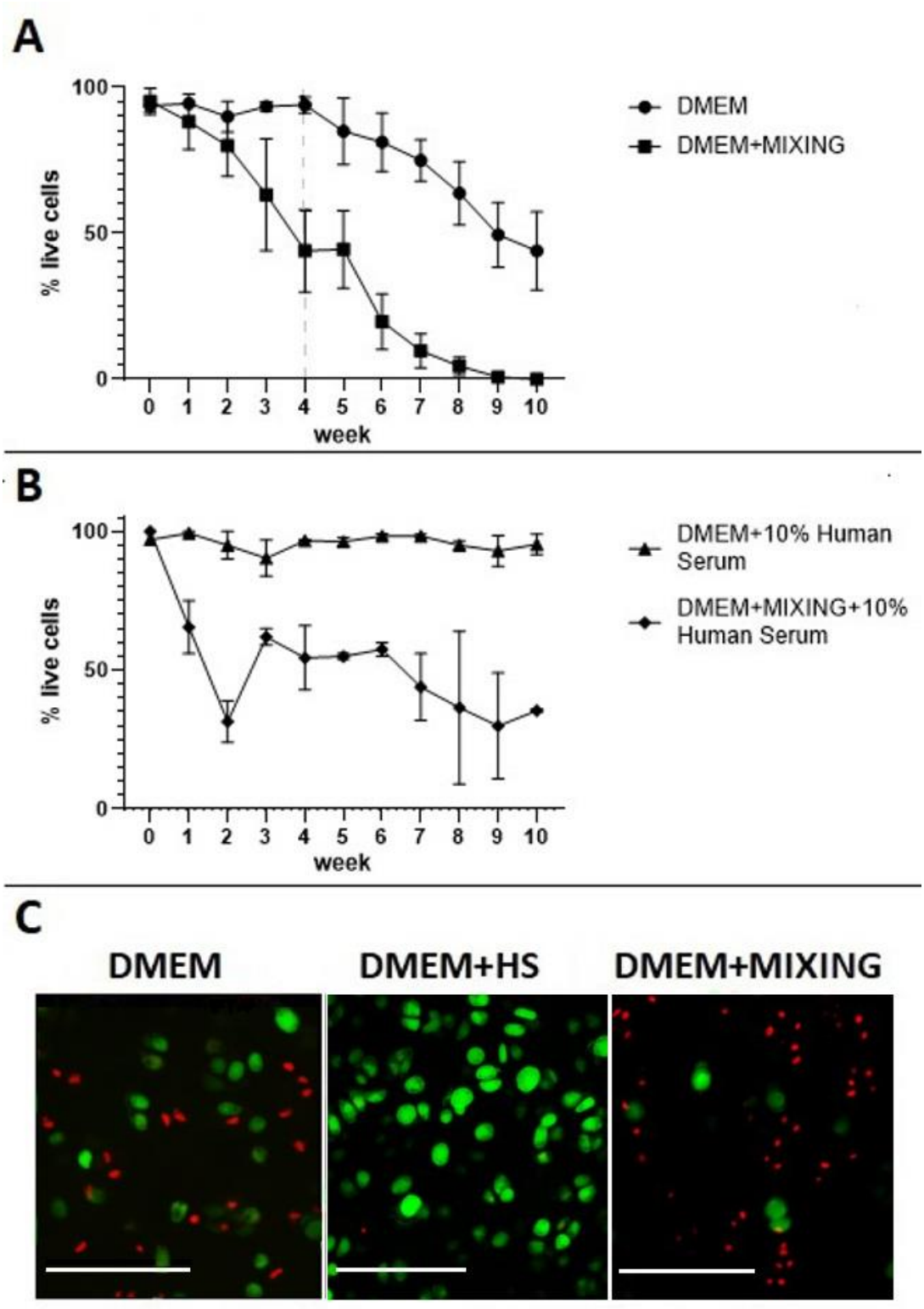

687
688

689 Figure 4.
690
691 (Styczynska-Soczka et al., 2020)
692

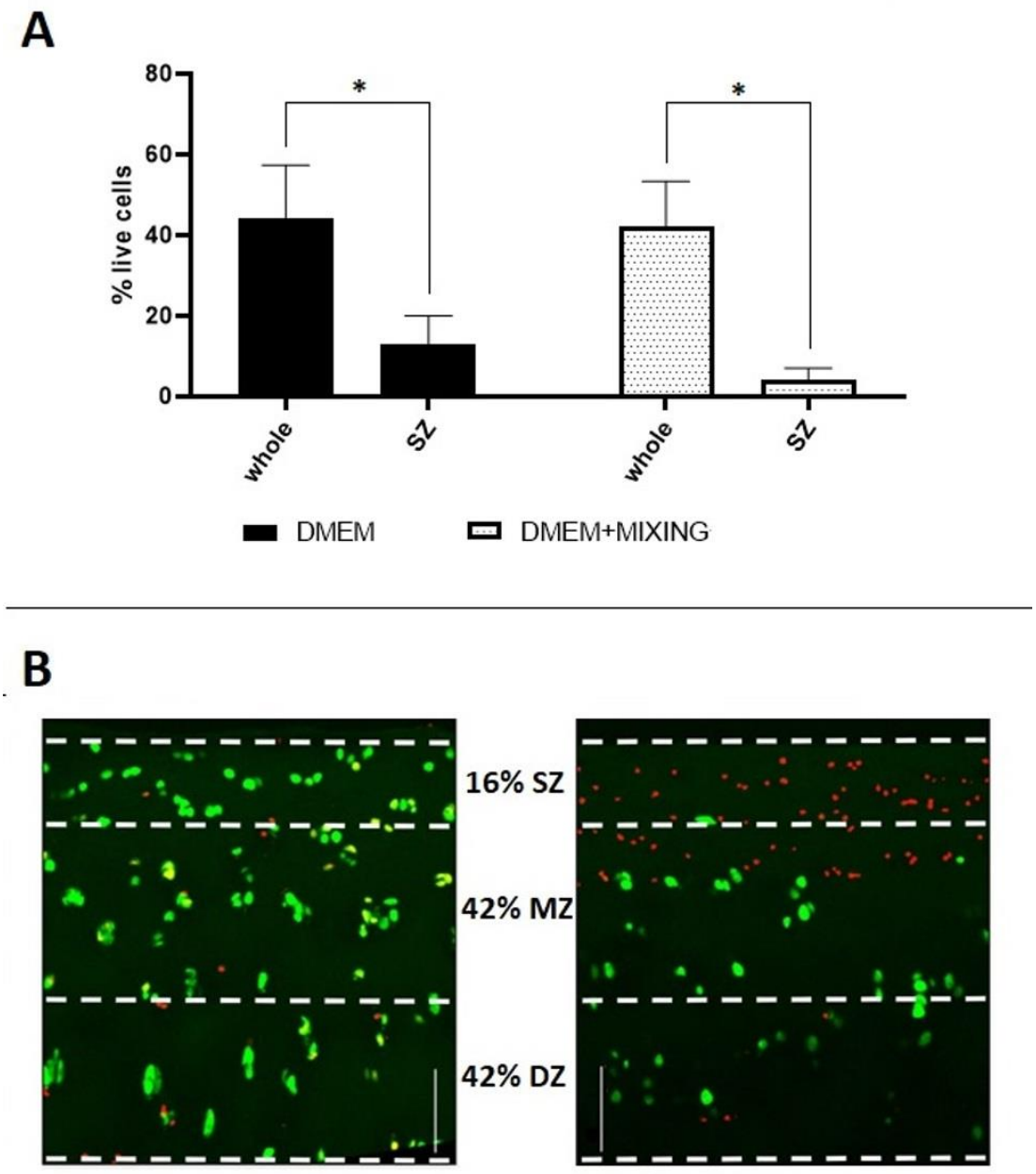

693
694
695
696

Figure 5.

(Styczynska-Soczka et al., 2020)

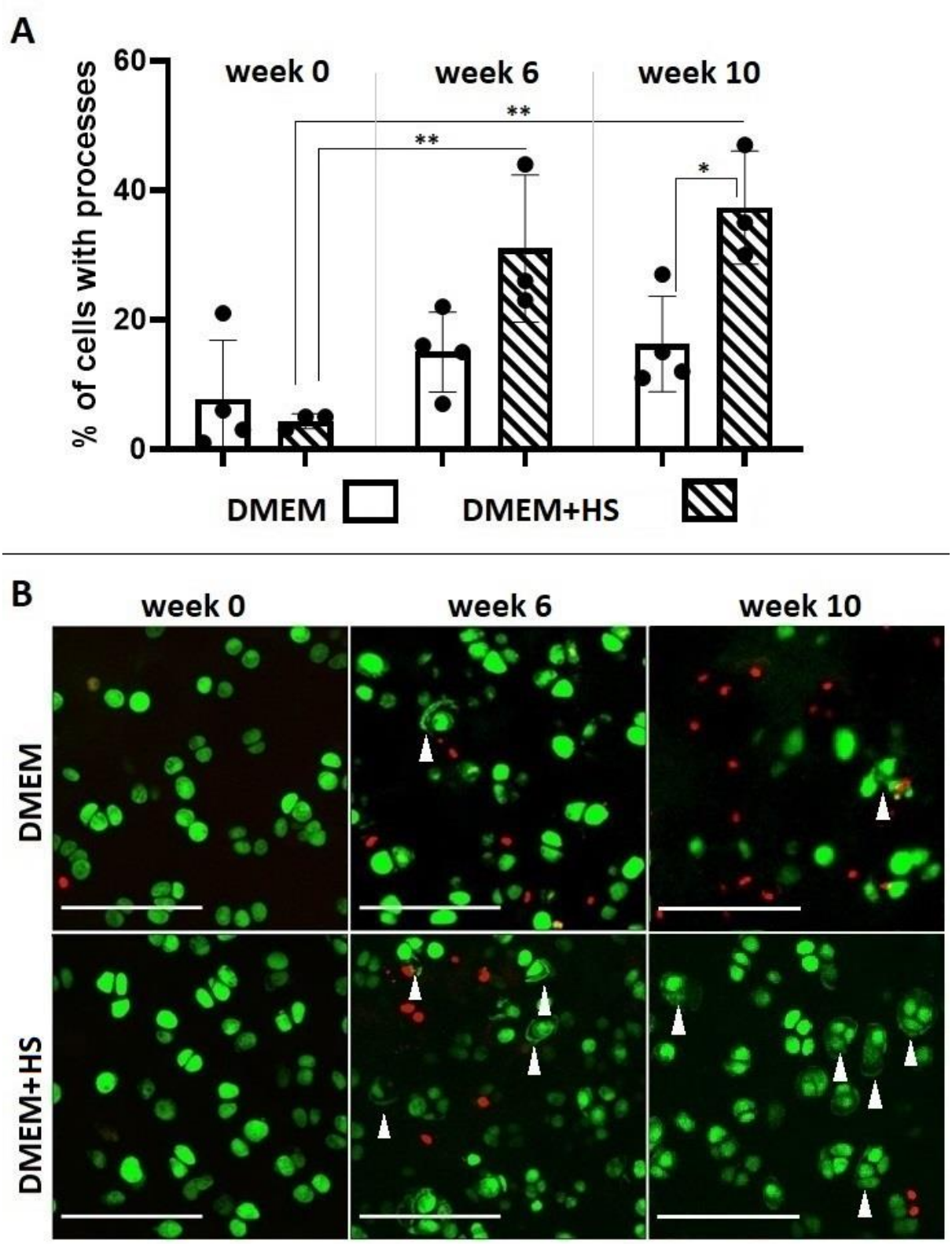

Figure 6.

(Styczynska-Soczka et al., 2020)

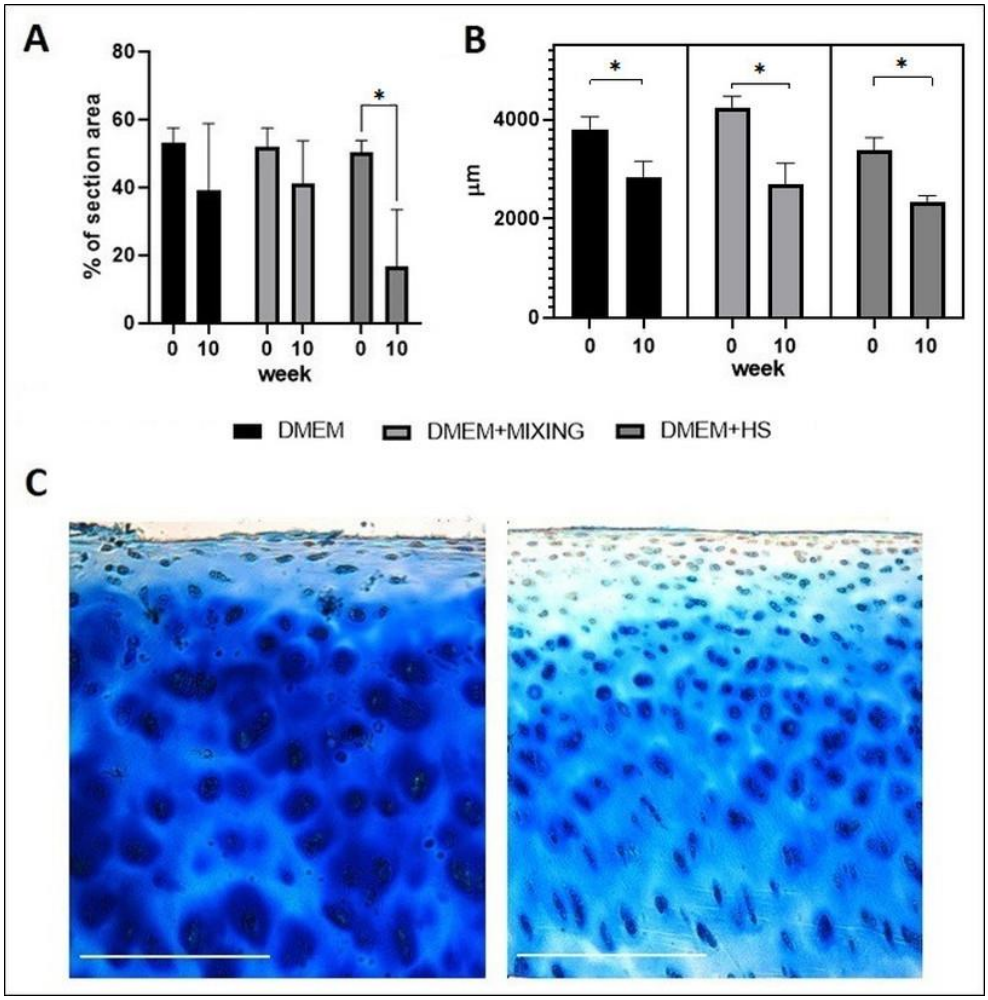

Figure 7.

(Styczynska-Soczka et al., 2020)